American Journal of Engineering Research (AJER)
e-ISSN : 2320-0847 p-ISSN : 2320-0936
Volume-02, Issue-09, pp-140-161
www.ajer.org

Research Paper Open Access

MHD Natural convection in the localized heat sources of an inclined trapezoidal Nanofluid-filled enclosure

M. A. Mansour, A.Y. Bakier, M. A. Y. Bakeir
Department of Mathematics, Faculty of Sciences, Assiut University, Assiut, Egypt

Abstract: - The effects of magnetic force, acting vertically downward on natural convection within a nanofluid filled tilted trapezoidal enclosure saturated with an electrically conducting fluid have been investigated numerically. The bottom wall of the enclosure is subjected to a constant cold temperature and the top wall experiences a heat source whereas the remaining sidewalls are kept adiabatic. The physical problems are represented mathematically by different sets of governing equations along with the corresponding boundary conditions. By using approximations of finite difference method, the non-dimensional governing equations are discritized. For natural convection the influential parameters are Rayleigh number Ra, the rotational angle of the enclosureΦ and the Hartmann number Ha, through which different thermo-fluid characteristics inside the enclosure are obtained. In the present study, the obtained results are presented in terms of streamlines, isotherms and average Nusselt number along the heat source. The result shows that with increasing Ha, the diffusive heat transfer become prominent even though Rayleigh number increases. Optimum heat transfer rate is obtained at higher values of Ra in the absence of magnetic force.

Keywords: - *magneto-hydrodynamics, inclination angle, nanofluid, Rayleigh number, solid volume fraction.*

I. INTRODUCTION

Magnetohydrodynamic (MHD) flow and especially when associated with heat transfer have received considerable attention recent years because of their wide variety of application in engineering areas such as crystal growth in liquid, cooling of nuclear reactor, electronic package, microelectronic devices, solar technology, etc. in case of free convection of an electrically conducting fluid in presence of magnetic field, there are two body force, buoyancy force and Lorentz force. They interact with each other an influence on heat and mass transfer, so it is important to study the detailed characteristics of transport phenomena in such a process to have a better product with improved design. A porous medium consists of a solid matrix with an interconnected void. This solid matrix is either rigid or deformable [1-2]. Porous materials such as sand and crushed rock underground saturated with water, which, under the influence of local pressure gradients, migrates and transports energy through the material. Natural convection heat transfer in a cavity saturated with porous media in the presence of magnetic field is a new branch of thermo-fluid mechanics.

The heat transport phenomenon can be described by means of the hydrodynamics, the convective heat transfer mechanism and the electromagnetic field as they have a symbiotic relationship [3–7]. The flow within an enclosure consisting of two horizontal walls, at different temperatures, is an important circumstance encountered quite frequently in practice. In all the applications having this kind of situation, heat transfer occurs due to the temperature difference across the fluid layer, one horizontal solid surface being at a temperature higher than the other. If the upper plate is the hot surface, then the lower surface has heavier fluid and by virtue of buoyancy the fluid would not come to the lower plate. Because in this case the heat transfer mode is restricted to only conduction. But if the fluid is enclosed between two horizontal surfaces of which the upper surface is at lower temperature, there will be the existence of cellular natural convective currents, which are called as Benard cells. For fluids whose density decreases with increasing temperature, this leads to an unstable situation. Benard [8] mentioned this instability as a “top heavy” situation. In that case fluid is completely stationary and heat is transferred across the layer by the conduction mechanism only. Rayleigh [9] recognized that this unstable situation must break down at a certain value of Rayleigh number above which convective motion must be

generated. Jeffreys [10] calculated this limiting value of Ra to be 1708, when air layer is bounded on both sides by solid walls.

The symbiotic interaction between the fluid velocity field and the electromagnetic forces give rise to a flow scenarios; the magnetic field affects the motion. Natural convection in an enclosure saturated with porous medium plays a significant role in many practical applications. Among those, geophysical systems: heat exchange between soil and atmosphere, dynamics of terrestrial heat flow through aquifer; compacted beds for the chemical industry, high performance insulations for cryogenic containers, sensible heat storage beds, food processing, grain storage, solar power collectors, flows over heat exchanger pipes, cooling of electronic systems, cooling of radioactive waste containers and the post-accidental heat removal in nuclear reactors have become increasingly important to the engineers and scientists. In this analysis, the effects of permeability and different thermal boundary conditions on the natural convection in a square porous cavity by using Darcy–Forchheimer model [11] and Darcy–Brinkman-Forchheimer model [12, 13] have been studied numerically. The tilted position of the enclosure [14–16] has a significant influence on the natural convection. Mahmud and Fraser [17] examined the flow, temperature and entropy generation fields inside a square porous cavity under the influence of magnetic field using Darcy model. The momentum equation including Navier–Stokes inertia term and Brinkman viscous diffusion term derived for the porous media in the presence of magnetic field makes the present works discernible. The main attribute for choosing the trapezoidal shape cavity is to enhance the heat transfer rate as it could be said intuitionally due to its extended cold top surface. Contextually the present study will focus on the computational analysis of the influence of magnetic field on the natural convection in a trapezoidal enclosure saturated with porous medium of constant porosity.

Nanotechnology has been widely used in industry since materials with sizes of nanometers possess unique physical and chemical properties. Nano-scale particle added fluids are called as nanofluid which is firstly introduced by Cho [18]. Use of metallic nanoparticles with high thermal conductivity will increase the effective thermal conductivity of these types of fluid remarkably. Because nanofluid consists of very small sized solid particles, therefore in low solid concentration it is reasonable to consider nanofluid as a single phase flow [19]. There are many numerical studies on natural convection flow of nanofluid in different geometries. The computational studies are much disputed, because the majority results have reported an enhancement in heat transfer due to the presence of nanoparticles [20–23]. It seems that the first numerical study of natural convection of Copper (Cu)–water nanofluid in a two dimensional enclosure was done by Khanafer et al. [20]. The nanofluid in the enclosure was assumed to be in single phase. It was found that for any given Grashof number, the average Nusselt number increased with the solid volume concentration parameter. Mahmoudi et al. [21] investigated numerically the effect of position of horizontal heat source on the left vertical wall of a cavity filled with Cu–water nanofluid. Their results showed that the presence of nanoparticles at low Ra was more pronounced; also when the heat source was located close to the top horizontal wall, nanofluid was more effective. Oztop and Abu-Nada [22] considered natural convection in partially heated enclosures having different aspect ratio and filled with nanofluid. They found that the heat transfer was more pronounced at low aspect ratio and high volume fraction of nanoparticles. Aminossadati and Ghasemi [23] considered the effect of apex angle, position and dimension of heat source on fluid flow and heat transfer in a triangular enclosure using nanofluid. They found that at low Rayleigh numbers, the heat transfer rate continuously increases with the enclosure apex angle and decreases with the distance of the heat source from the left vertex. Natural convection in trapezoidal enclosures has been the subject of interest for many studies due to its important application in various fields such as electronic components and solar collectors. Although, there are some valuable studies on natural convection in trapezoidal enclosures using pure fluid [24–26], only a few works considered the effect of nanofluid [27, 28]. But no attempt was made to optimize the problem. This can be done by using the Entropy Generation Minimization technique as introduced by Bejan [29]. However, there are only a few studies that consider the second thermodynamic laws in the presence of nanofluids [30–31]. Shahi et al. [30] numerically studied the entropy generation and natural convection in a square cavity with a vertical heat source which is filled with copper–water nanofluid. They have considered entropy generation and heat transfer for a wide range of the Rayleigh number, solid volume fraction parameter and different positions of the heat source. The present study will focus on the computational analysis of the influence of magnetic field on the nanofluid in natural convection in a tilted trapezoidal enclosure saturated with porous medium of constant porosity.

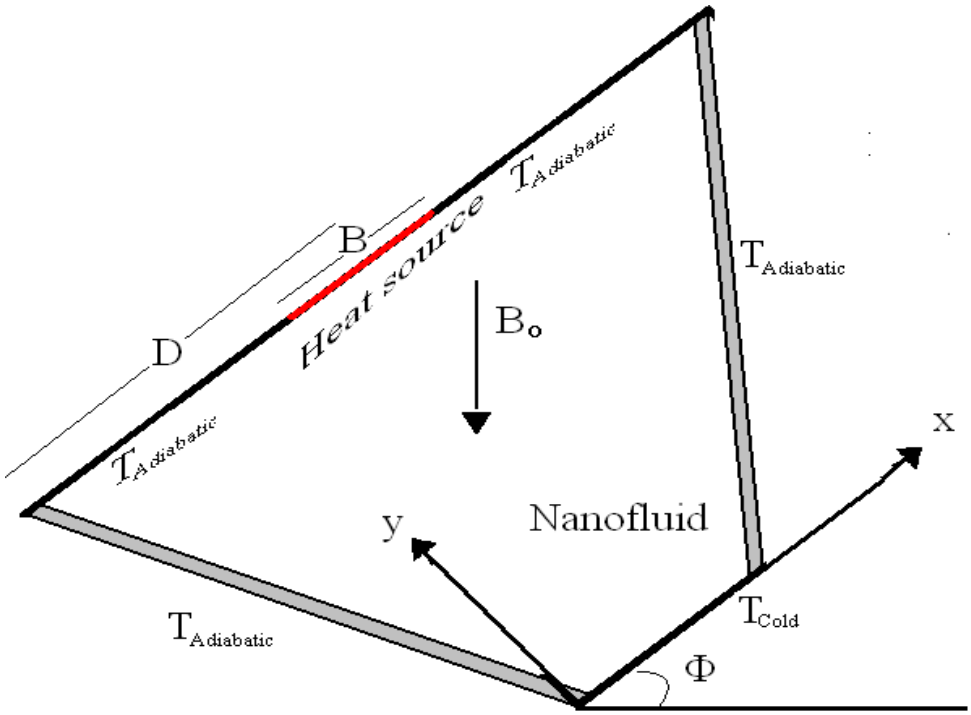

Fig. 1. Schematic diagram of physical problem.

II. MATHEMATICAL MODEL

Fig. 1 shows the flow model used. Consider same assumptions mentioned, then the governing equations of momentum is deducted as (Mamun et al. (2010), Basak et al. (2009) and Mansour et al. (2010)). Moreover, using the same dimensionless transforms (Eq. (12)); the governing equations can be formulated as:

Continuity equation,

$$\frac{\partial U}{\partial X}+\frac{\partial V}{\partial Y}=0 \tag{1}$$

Momentum equation,

$$\frac{\partial \psi}{\partial y}\frac{\partial \Omega}{\partial X}-\frac{\partial \psi}{\partial x}\frac{\partial \Omega}{\partial Y}=\frac{\mu_{nf}}{\rho_{nf}\alpha_f}\left(\frac{\partial^2\Omega}{\partial X^2}+\frac{\partial^2\Omega}{\partial Y^2}\right)$$
$$+Ha^2\,\mathrm{Pr}\frac{\sigma_{nf}}{\sigma_f}\frac{\rho_f}{\rho_{nf}}\left[\cos\Phi\frac{\partial^2\psi}{\partial Y^2}+\sin\Phi\frac{\partial\psi}{\partial Y\partial X}\right]$$
$$+Ra\,\mathrm{Pr}\frac{\rho_f}{\rho_{nf}}\left[1-\varphi+\frac{(\rho\beta)_s}{(\rho\beta)_f}\varphi\right]\left(\cos\Phi\frac{\partial\theta}{\partial Y}+\sin\Phi\frac{\partial\theta}{\partial X}\right) \tag{2}$$

Where Ha (= $\beta_0 W(\sigma/\mu)^{0.5}$) is Hartmann number, σ electrical conductivity and Φ is the inclination angle.

$$\Omega=\frac{\partial V}{\partial X}-\frac{\partial U}{\partial Y}=-\nabla^2\psi \tag{3}$$

$$\frac{\partial \psi}{\partial Y}\frac{\partial \theta}{\partial X}-\frac{\partial \psi}{\partial X}\frac{\partial \theta}{\partial Y}=\frac{\alpha_{nf}}{\alpha_f}\left(\frac{\partial^2\theta}{\partial X^2}+\frac{\partial^2\theta}{\partial Y^2}\right) \tag{4}$$

The boundary conditions are

Bottom wall : $\psi=0,\theta=0$ (5 a)

Top wall : $\psi=0,\theta=1;\ D-B/2<X<D+B/2$ (5 b)

Otherwise : $\psi=0,\frac{\partial\theta}{\partial n}=0$ (5 c)

Sides' walls: $\psi = 0, \frac{\partial \theta}{\partial n} = 0$ (5 d)

where *n* is a vector perpendicular to the side wall.

Numerical method and validation

Equations (1)-(4) subject to the boundary conditions (5) are solved numerically by using the finite difference methodology. Then all these analyses are implemented in a FORTRAN program. The solution procedure is iterated until the following convergence criterion is satisfied:

$$\sum_{i,j} | \chi_{i,j}^{new} - \chi_{i,j}^{old} | \leq 10^{-7}$$

where χ is the general dependent variable. Prior to the simulations (Ching-Chang Cho et al., 2012), a grid –independence analysis has been performed to determine the mesh size which achieved the optimal compromise between the computational cost of the solution procedure and the numerical accuracy.

The finite difference method uses four sets of grids: 882, 1922, 3362, and 5202. There is a good agreement was found for 1922 nodes as shown in table 1. In order to verify the accuracy of present method, the obtained results in special cases are compared with the results obtained by Walker and Homsy (1978), Gross et al. (1986), Manole and Lage (1992). Table 3 shows a good agreement was found between the present results and the results obtained by the previous works in the test case. These favorable comparisons lend confidence in the numerical results to be reported subsequently.

Table 1 Grid independency results

	Nu_m	θ_{max}	ψ_{max}	ψ_{min}
882	5.602	0.183	0.682	-1.290
1922	5.593	0.185	0.706	-1.292
3362	5.768	0.181	0.777	-1.292
5202	6.054	0.173	0.877	-1.292

Table 2. Thermo-physical properties of water and nanoparticles.

	Pure water	Copper (Cu)
$\rho(kgm^{-3})$	997.1	8933
$C_p(Jkg^{-1}K^{-1})$	4179	385
$k(Wm^{-1}K^{-1})$	0.613	401
$\beta(K^{-1})$	21×10^{-5}	1.67×10^{-5}
σ	0.05	$5.96\text{x}10^{7}$

Table 3. Comparison of ψ_{max}.

Ra	Haajizadeh et al. [38]	Grosan et al. [36]	Present
	ψ_{max}	ψ_{max}	ψ_{max}
10	0.078	0.079	0.0799
10^3	4.880	4.833	4.8266

III. RESULTS AND DISCUSSION

Metamorphosis of thermo-fluid fields have described. There exists a counter circulating cell in Fig. 2, where the core of the vortex lays in the left upper region of the cavity near the heat source, D=-0.5, and therefore fluid has crowded in the left half of the enclosure. As the inclination angle increases, the fluid motion increases which mean the obvious effect of buoyancy force. Hydrodynamic boundary layer along all walls except for the right inclined sidewall. Isotherms are polarized in the left-upper corner. Therefore the thermal boundary layer is very small in the inclined sidewall. It's observed stratification for temperature field. The effect of magnetic force is multiple with buoyancy force because they experience in the same direction. For inclination angle greater than 45° the flow tends to stretch diagonally. Fig. 3 shows the nano case; the hydro-field for circulating cell has been zoned from the extreme left-upper corner due to the existence of nanoparticles through the fluid, and the geometric attributes for this corner. It can be observed a week rotation clockwise has been formed as a counter effect of duple governing force which producing the circulating cells extensively regions in

the cavity. So in this corner the viscous force is prominent. As the inclination angle increases, the resultant force decays because the buoyancy force is not being still work at the same destination of magnetic force. Thereby the effect of viscous force has been destroyed. Increasing of the inclination angle the primary circulation cell are stretching diagonally until it is becoming 90 where the magnetic force is perpendicular to buoyancy force. The buoyancy force gets the flow move upward for away from the left-upper corners. On other hand, Ha generates the viscous diffusion flow. These two phenomena make three circulating cells, the strength of them increases as flow moves toward the right side. Flow comes from the cold wall to hot wall thereby diffusion currents are overwhelmed by convection currents. The extreme left portion resulting good thermal performance, while the extreme right region represents diffusion dominated zone where the motion is very strong since it's only subjected to the normal magnetic field. It's noticed that there are two circulating cells in the ends which are in the anti-clockwise direction, so that the circulating cell entrapped with them is in the clockwise direction. By continue, the primary vortex grasps with other circulating cells. All of them expand paralleling to the secondary diagonal direction. Temperature keeps invariant during the round. Until the angle = 90, a huge disturbance happens because of the appearance of diffusion heat transfer in the right part. The effects of heat source location, heat source length and Hartmann number are showed in Figs. 4-6. The core of vortex follows D's movement it is noticeable there is no similarity even if the heat source location in the bisection way because Ha effect is regular along the top surface. In the same direction the effect buoyancy force acting from the source. It is observed the similarity between each pairs of corresponding cases such as the two cases of D=-0.5 and 1.5. As B increases the circulating cell has stretched horizontally and then the hydrodynamic boundary layer decreases. Also the stratification in the isotherms increases indicating the strong influence of viscous diffusion. It is observed that the temperature gradients increase as B increases at the vicinity of tilted left surface, where the inclination angle =45 the thermal boundary layers very tinny along this surface invoking the supremacy of convection heat transfer. For low Ha the motion is regularly at whole the cavity where a singular circulating cell and counter clockwise direction of motion. As Ha increases the circulating cell squeezes toward the nearest side to the heat source. Because the intensity of magnetic force increases the resulting recirculation cell experience the retarding motion. The diffusion current starts to dominate the convection current. As the magnetic force triumphs over buoyancy force, the core of the vortex shifts toward the source. By increasing of Ha, a core of circulating cell is shifted resulting formulation a stagnation point in the left upper corner. Also, temperature lines switch toward the left side decelerating the formulation of thermal boundary layer. At Ha =100, multicellaur formulation is appeared in the cavity. The weaker zone is shifted and the major vortex is entrapped by two minor vortices so the diffusion flow becomes more prominent. The oscillating thermal boundary layer represents the dominancy of diffusion heat flux. Figs. 7-9 display the effect of Ha, D and B in the nano case. The symmetry in streamlines in Fig. 7 which appears two contour rotating vortices is due to symmetrical dynamic flow and symmetrical boundary condition. At the absence of magnetic force the strength of circulating cell is high relatively. Thermal boundary layer in the left side has more effect than the right side. As Ha increases the core of vortex stretched toward the source. Increasing Ha also leads to increase temperature gradient and increase heat transfer rate consequently. Comparing with Fig. 4, considering the change in the inclination angle, it is observed the relation between D and buoyancy force which appears its effect in generation of vortices and the relation between D and temperature gradient reflecting the effective range of diffusion heat transfer and size of thermal boundary layer. Variation of B explains the link between heat source and the idiosyncratic attributes for thermo-flow application. As B increases the fluid motion tends to take the anti-clockwise direction, therefore at B=2 there exists three cores. Two of them are produced by the stretch happening in the counter circulation cell. For isotherms, the changing of B is related to the stratification of temperature lines which ensures the dominancy of diffusion heat transfer. For moderate value of Ha=5, Figs 10 and 11 show the effect of solid volume fraction in various titled positions. By studying the scenario of change horizontally, it confirms the argument of Fig. 2 the vertically studying, for the familiar position the increase of solid volume fraction get the flow more be symmetric. But for other inclination positions, it is observed a shipment of core of vortices are generated and rigorous develop of plumage has been happened. The left circulating cell decays and minor vortices have grasped to the major vortex which expanded diagonally. Isotherms tend to cluster in the right portion as the inclination angle increases respect to the buoyancy force. The vertical scenario shows that the increase of the angle leads to increase the diffusion current. For Figs. 12 and 13, increases in Ha result in increase the polarization of the core of circulating cells toward the source, which appears by horizontal change. Also it leads to increase the diffusion current adding to convection current. The vertical scenario shows at the absence of magnetic force, increasing in Ra makes the flow unsymmetrical. Also it strengthens the counter circulation cell and increases the convection heat transfer. Fig. 14 shows the symmetrical behavior of local Nusselt number. As B decreases, the heat transfer rate increases, moreover, the temperature gradients increases. Fig. 15 offers the symmetrical behavior of Nu –local- around the D, which strengthens the heat transfer rate. Figs 16 and 17 ensure the previous argument about Figs. 14 and15. It shows

the effect of inclination angle on the heat transfer generally. Fig. 18 deduces that Nu_m slightly decreases as the solid volume fraction increases except for B=0.2 because the greatest value of temperature gradient and heat transfer rate. It is showed that Nu_m increases as B decreases. Fig. 19 and 20 show the average Nusselt number increases with the solid volume fraction for constant parameters' motion except for Ha which decreases the Nu_m. When Ra is the only variable in the Nu_m-φ relation, Nu_m increases linearly with φ and Ra enhances it. As the inclination angle increases in Fig. 21, Nu_m increases. The relation between Nu_m-φ is irregular; however Nu_m increases with φ linearly for the small angles. Nu_m increases with Ra as an exponentially behavior in Fig. 22 where Ra changes in logarithm way. Ha do not affect Nu_m for small Ra; otherwise, it has a huge effect for high Ra values. Figs. 23 -27 show relations V-X and temperature-X. Vertical velocity tends to be symmetrical for { φ, B , Ha} changes, while temperature tends to be more smooth for both Ha and Ra changes. At X=0.5, the maximum value for velocity when Ha=0 while for temperature when Ha=20. The global maximum temperature at B=2.

IV. CONCLUSION

Magneto-hydrodynamics (MHD) is the science of the motion of electrically conducting fluids under the influence of applied magnetic forces. A numerical study has been achieved for the natural convection cooling of a heat source mounted inside a trapezoidal cavity filled by Cu–water nanofluid in the presence of vertical magnetic field. It was observed that the increasing in inclination angle enhances the buoyancy force while the effect of viscous force has been vanished. At maximum inclination angle, the left part of the enclosure has good thermal performance but the right represents diffusion dominated zone where the motion is subject to the magnetic force. Increase of B produces a strong influence of viscous diffusion. In the left inclined surface, once the inclination angle equal 45 the flow invokes the supremacy of convection heat transfer. As Ha increases the temperature gradients increases, hence heat transfer rate increases. At Ha=100 the oscillating thermal boundary layer refers to the dominancy of diffusion heat flux. There is a strong relation between the heat transfer location and the temperature gradient in nanofluid which reflects the effective range of diffusion heat transfer and size of thermal boundary layer. It is noticed that as the solid volume fraction increases the diffusion currents increase. But as Ra increases the convection currents increase specially in the absence of magnetic force.

REFERENCES

[1] M.A.H. Mamun, Md.T. Islam, Md.M. Rahman, Natural convection in a porous trapezoidal enclosure with magneto-hydrodynamic effect, Nonlinear Analysis: Modelling and Control, 2010, Vol. 15, No. 2, 159–184.

[2] J. Bear, Dynamics of Fluids in Porous Media, American Elsevier publishing company, Inc., New York, 1972.

[3] D.A. Nield, A. Bejan, Convection in Porous Media, 3rd ed., Springer, New York, 2006.

[4] Transport Phenomena in Porous Media, D.B. Ingham, I. Pop (Eds.), Elsevier, Oxford, 2005.

[5] Hanbook of Porous Media, K. Vafai (Ed.), 2nd ed., Taylor & Francis, Boca Raton, 2005.

[6] Emerging Topics in Heat and Mass Transfer in Porous Media, P. Vadasz (Ed.), Springer, New York, 2008.

[7] I. Pop, D.B. Ingham, Convective Heat Transfer: Mathematical and Computational Modeling of Viscous Fluids and Porous Media, Pergamon, Oxford, 2001.

[8] H. B´enard, Formation p´eriodique de centres de giration `a l'arri`ere d'un obstacle en mouvement, C. R. Acad. Sci., 147, pp. 839–842, 1908.

[9] L. Rayleigh, On convection currents in a horizontal layer of fluid when the higher temperature is on the underside, Philos. Mag., 6(32), pp. 529–546, 1946.

[10] H. Jeffreys, Some cases of instabilities in fluid motion, P. Roy. Soc. Lond. A Mat., 118, pp. 195–208, 1928.

[11] N.H. Saied, I. Pop, Non-Darcy natural convection in a square cavity filled with a porous media, Fluid Dyn. Res., 36, pp. 35–43, 2005.

[12] F.Marcondes, J.M.Medeiros, J.M. Gurgel, Numerical analysis of natural convection in cavities with variable porosity, Numer. Heat Tr. A-Appl., 40, pp. 403–420, 2001.

[13] P. Nithiarasu, K.N. Seetharamu, T. Sundararajan, Numerical investigation of buoyancy driven flow in a fluid saturated non-Darcian porous medium, Int. J. Heat Mass Tran., 42, pp. 1205–1215, 1999.

[14] E. Baez, A. Nicolas, 2D natural convection flows in tilted cavities: Porous media and homogeneous fluids, Int. J. Heat Mass Tran., 49, pp. 4773–4785, 2006.

[15] A.C. Baytas, I. Pop, Natural convection in a trapezoidal enclosure filled with a porous medium, Int. J. Eng. Sci., 39, pp. 125–134, 2001.

[16] F.C. Lai, I. Pop, Natural Convection in a Truncated Circular Sector of Porous Medium, Int. Commun. Heat Mass, 17, pp. 801–811, 1990.
[17] S. Mahmud, R.A. Fraser, Magnetohydrodynamic free convection and entropy generation in a square porous cavity, Int. J. Heat Mass Tran., 47, pp. 3245–3256, 2004.
[18] Cho SUS. Enhancing thermal conductivity of fluids with nanoparticles. ASME Fluids Eng Division 1995;231:99–105.
[19] Xuan YM, Li Q. Heat transfer enhancement of nanofluid. Int J Heat Fluid Flow 2000;21:58–64.
[20] Khanafer K, Vafai K, Lightstone M. Buoyancy-driven heat transfer enhancement in a two-dimensional enclosure utilizing nanofluids. Int J Heat Mass Transfer 2003;46:3639–53.
[21] Mahmoudi AH, Shahi M, Raouf A, Ghasemian A. Numerical study of natural convection cooling of horizontal heat source mounted in a square cavity filled with nanofluid. Int Commun Heat Mass Transfer 2010;37:1135–41.
[22] Oztop HF, Abu-Nada E. Numerical study of natural convection in partially heated rectangular enclosures filled with nanofluids. Int J Heat Fluid Flow 2008;29:1326–36.
[23] Aminossadati SM, Ghasemi B. Enhanced natural convection in an isosceles triangular enclosure filled with a nanofluid. Comput Math Appl 2011;61:1739–53.
[24] Natarajan E, Basak T, Roy S. Natural convection flows in a trapezoidal enclosure with uniform and non-uniform heating of bottom wall. Int J Heat Mass Transfer 2008;51:747–56.
[25] Basak T, Roy S, Singh A, Balakrishnan AR. Natural convection flows in porous trapezoidal enclosures with various inclination angles. Int J Heat Mass Transfer 2009;52:4612–23.
[26] Varol Y, Oztop HF, Pop I. Natural convection in right-angle porous trapezoidal enclosure partially cooled from inclined wall. Int Commun Heat Mass Transfer 2009;36:6–15.
[27] Saleh H, Roslan R, Hashim I. Natural convection heat transfer in a nanofluid-filled trapezoidal enclosure. Int J Heat Mass Transfer 2011;54: 194–201.
[28] Nasrin R, Parvin S. Investigation of buoyancy-driven flow and heat transfer in a trapezoidal cavity filled with water–Cu nanofluid. Int Commun Heat Mass Transfer 2012;39:270–4.
[29] Bejan A. Entropy generation through heat and fluid flow. New York: Wiley; 1982.
[30] Mahmoudi AH, Shahi M, Talebi F. Entropy generation due to natural convection in a partialy open cavity with a thin heat source subjected to a nanofluid. Numer Heat Transfer A 2012;61:283–305.
[31] Shahi M, Mahmoudi AH, Honarbakhsh Raouf A. Entropy generation due to natural convection cooling of a nanofluid. Int Commun Heat Mass Transfer 2011;38:972–83.
[32] M. Mahmoodi, S. M. Hashemi, Numerical study of natural convection of a nanofluid in C-shaped enclosures, International Journal of Thermal Sciences 55 (2012) 76-89.
[33] Brinkman HC. The viscosity of concentrated suspensions and solutions. J. Chem. Phys. 1952;20:571–81.
[34] Maxwell JC. A treatise on electricity and magnetism. 2nd ed. Cambridge: Oxford University Press; 1904. p. 435–41.
[35] M.A. Mansour, A.J. Chamkha, R.A. Mohamed , M.M. Abd El-Aziz , S.E. Ahmed, MHD natural convection in an inclined cavity filled with a fluid saturated porous medium with heat source in the solid phase. Nonlinear Anal. 15(2010) 55–70.
[36] T. Grosan , C. Revnic, I. Pop, D.B. Ingham, Magnetic field and internal heat generation effects on the free convection in a rectangular cavity filled with a porous medium. Int. J. Heat Mass Transf. 52(2009)1525–1533.
[37] B.V. Ratish Kumar, P.V.S.N. Murthy, P. Singh, Free convection heat transfer from an isothermal wavy surface in a porous enclosure. Int. J. Numer. Meth. Fluids 28(1998) 633–661.
[38] M. Haajizadeh , A.F. Ozguc and C.L. Tien, Natural convection in a vertical porous enclosure with internal heat generation, Int. J. Heat Mass Transfer, 27(1984) 1893–190.

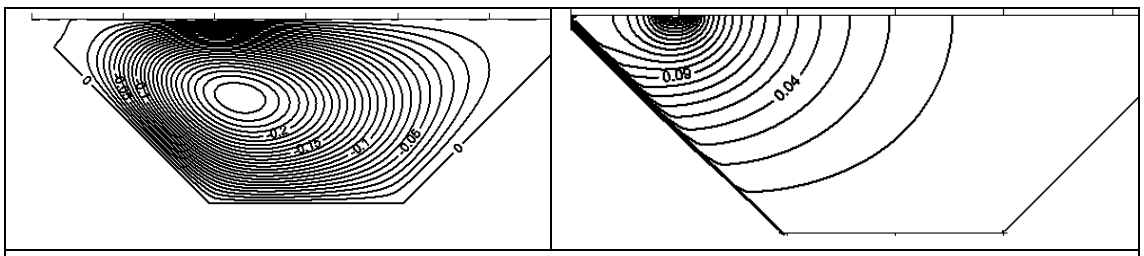

$\Phi = 0$

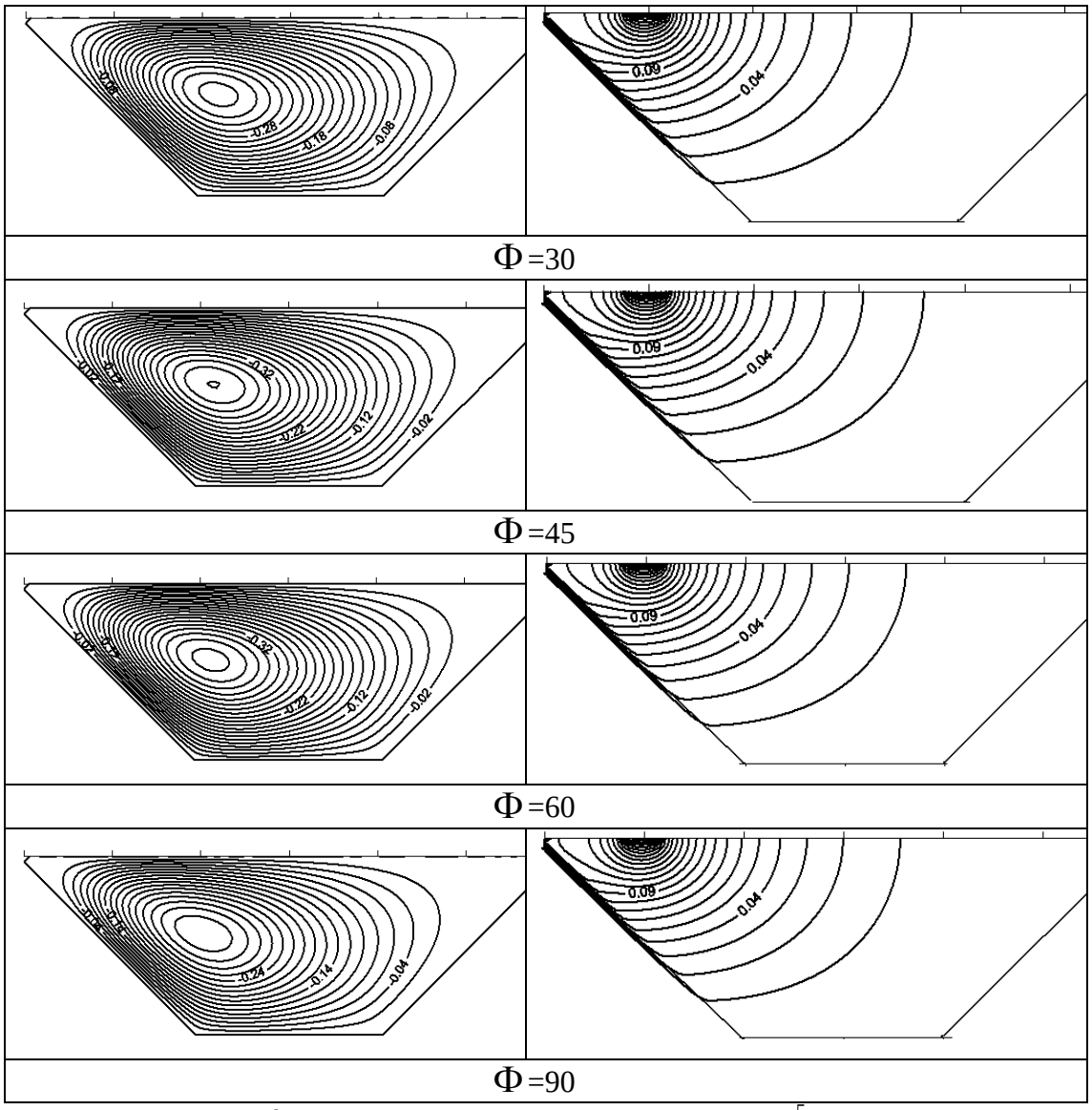

Fig 2 Streamlines (left) and isotherms (right) with Ha=5, Ra=10^5, B=0.2, D=-0.5, φ =0.

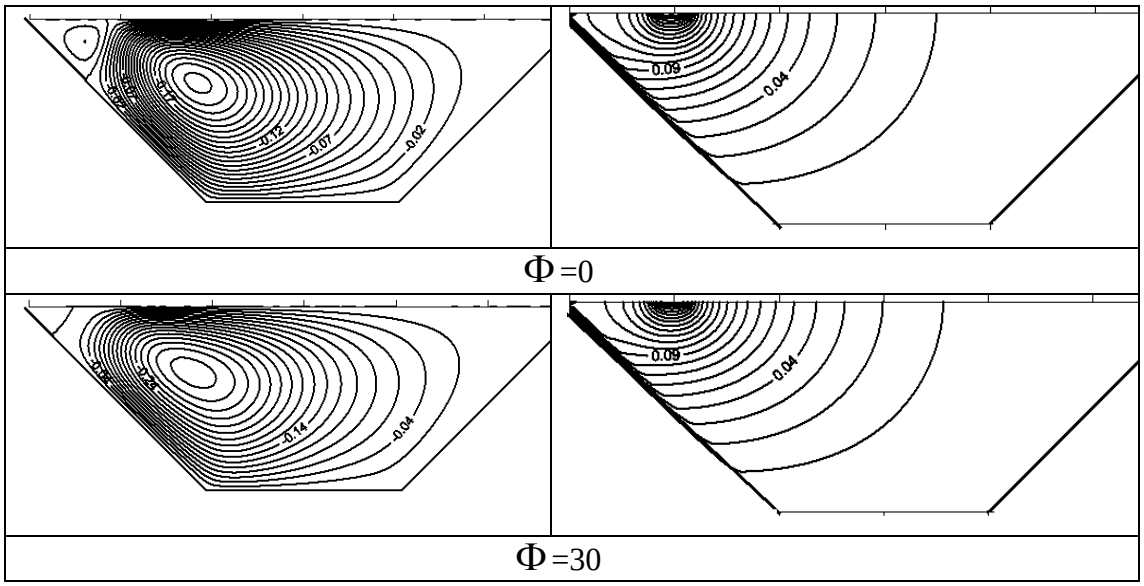

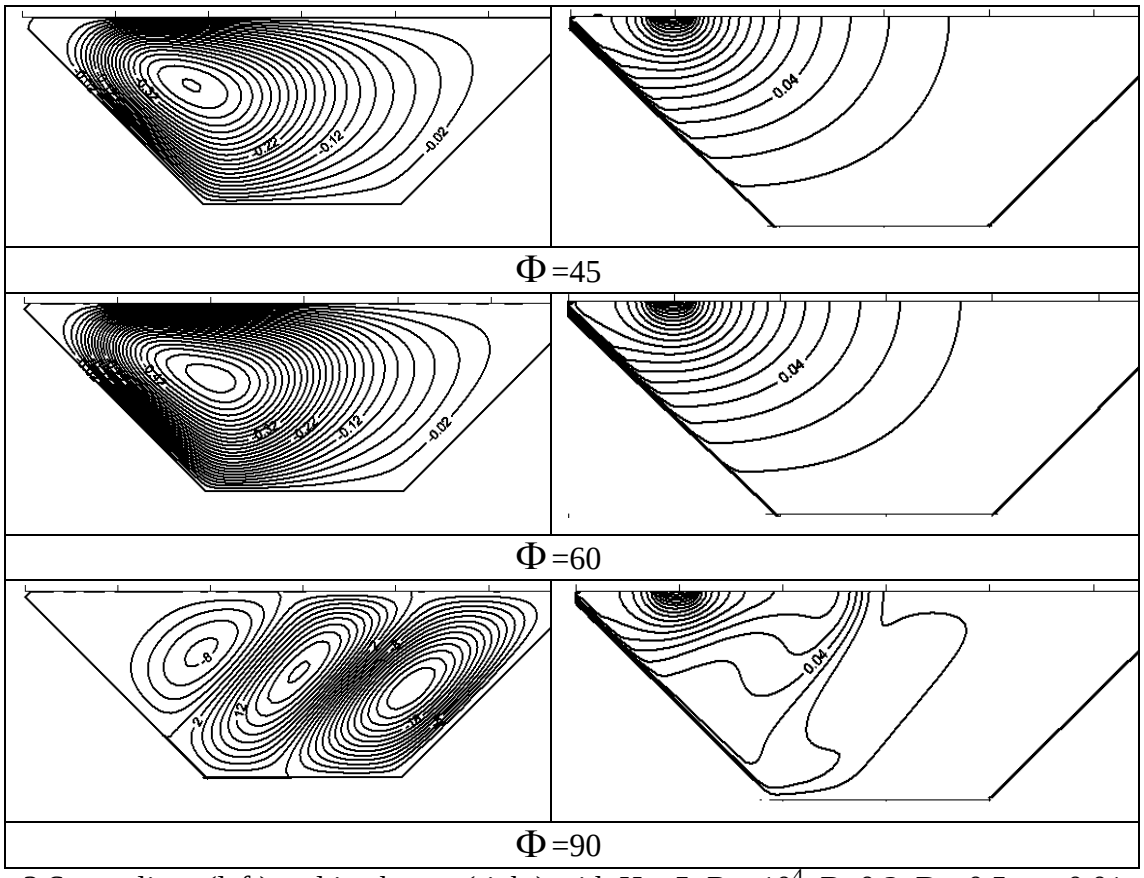

Fig 3 Streamlines (left) and isotherms (right) with Ha=5, Ra=10^4, B=0.2, D=-0.5, φ =0.01.

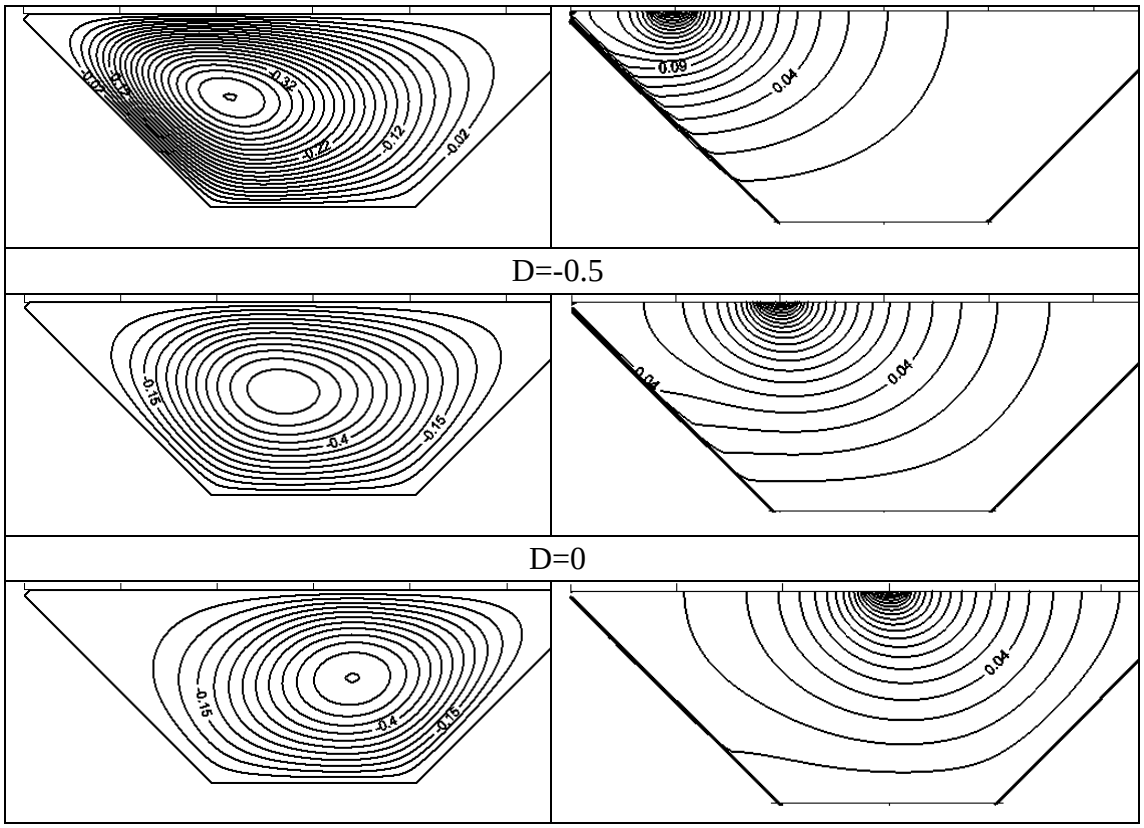

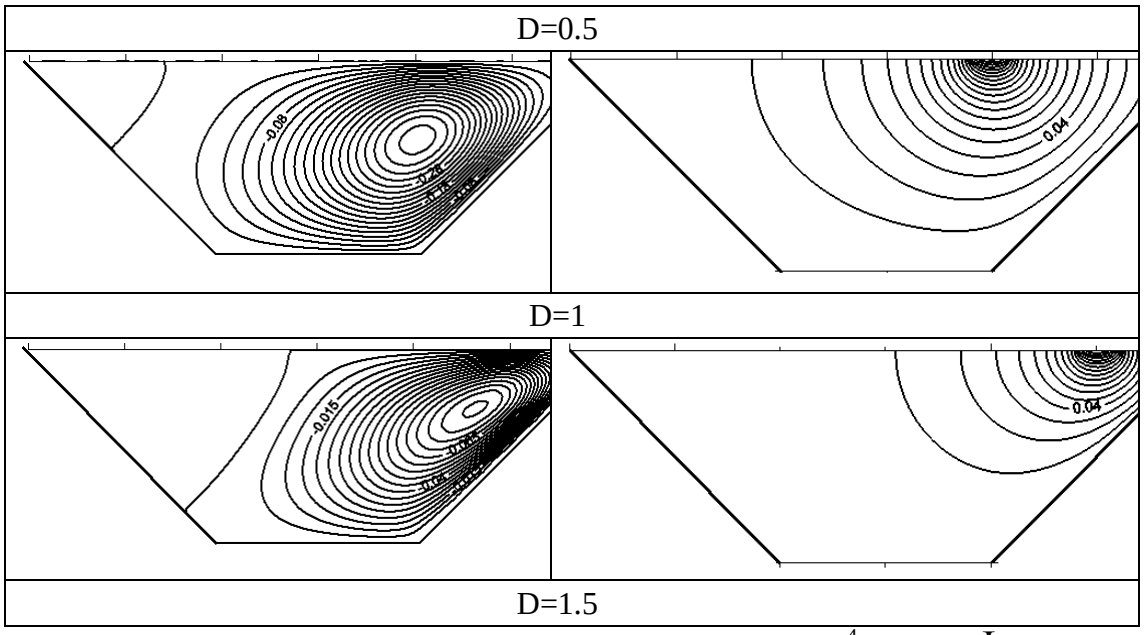

Fig 4 Streamlines (left) and isotherms (right) with Ha=5, Ra=10^4, B=0.2, Φ=45, φ=0.

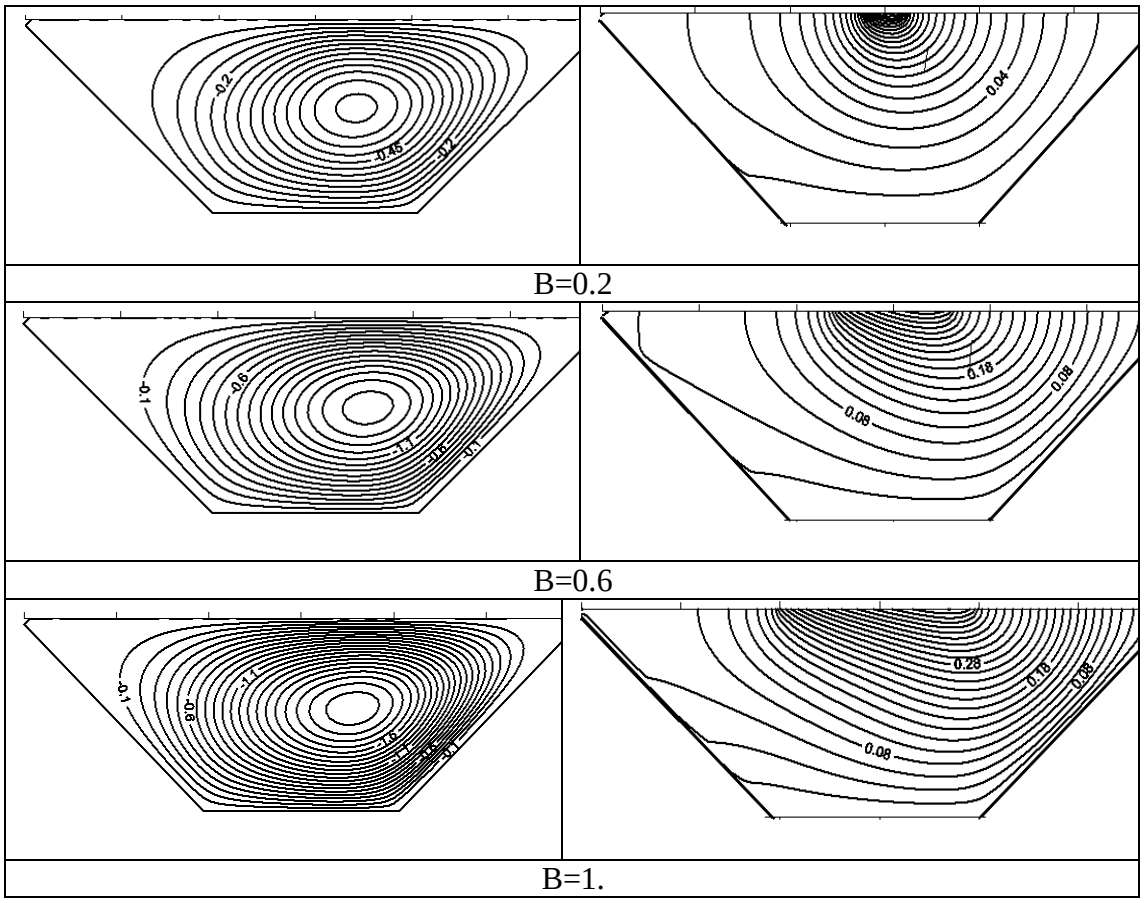

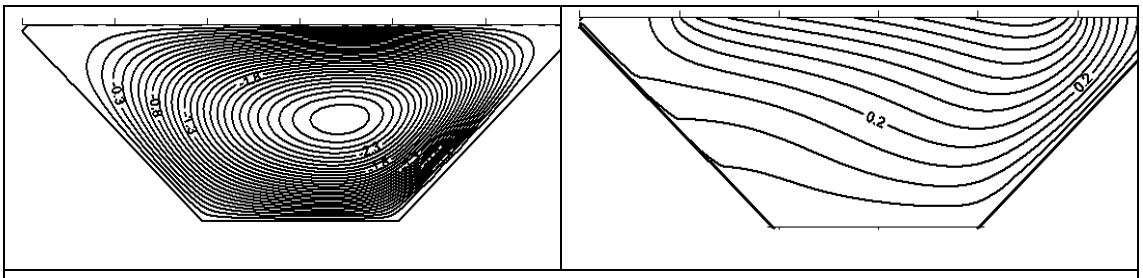

B=2.

Fig 5 Streamlines (left) and isotherms (right) with Ha=5, Ra=10^4, D=0.5, Φ=45, φ=0.

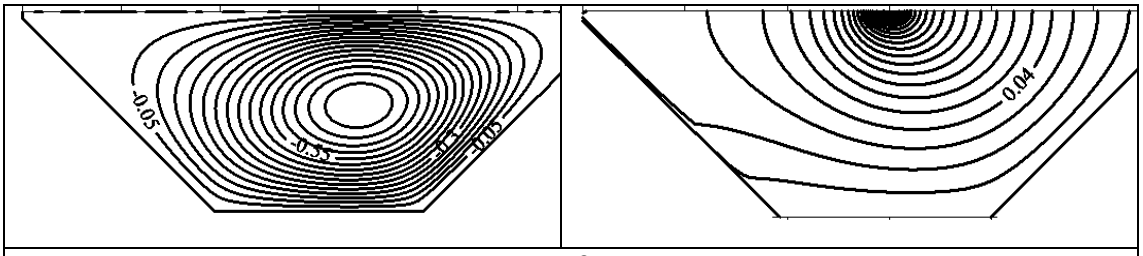

Ha=0

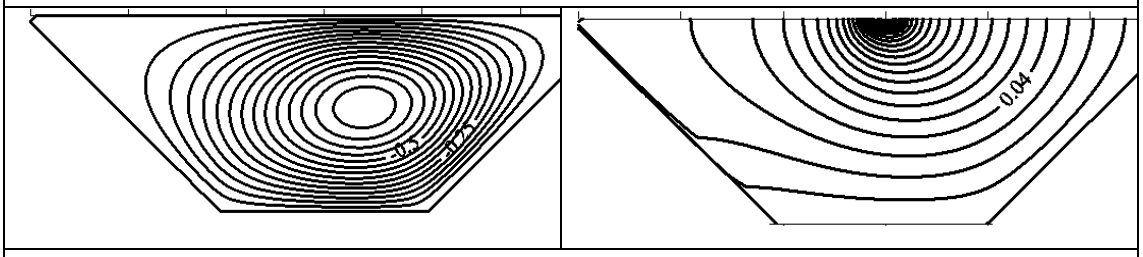

Ha=5

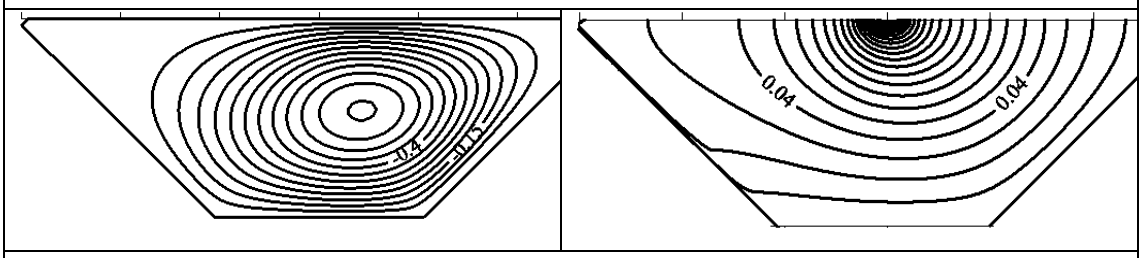

Ha=10

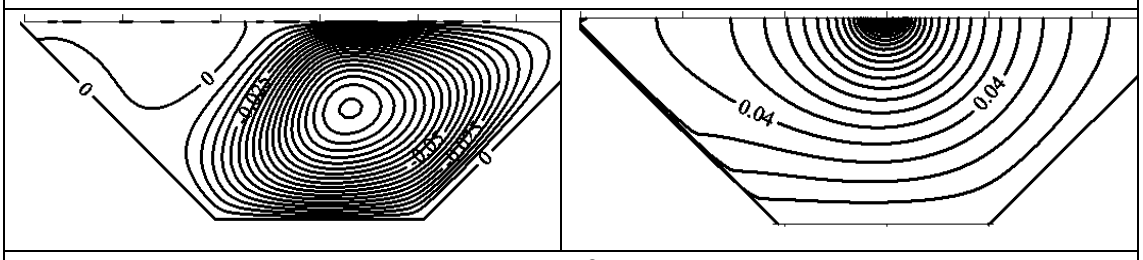

Ha=50

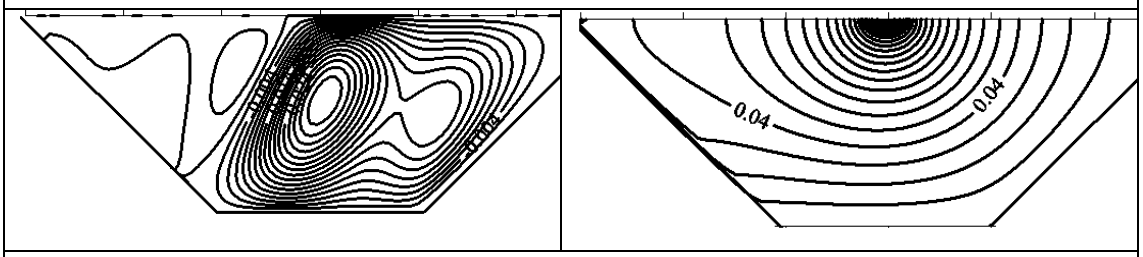

Ha=100

Fig 6 Streamlines (left) and isotherms (right) with B=0.2, Ra=10^4, D=0.5, Φ=45, φ=0.

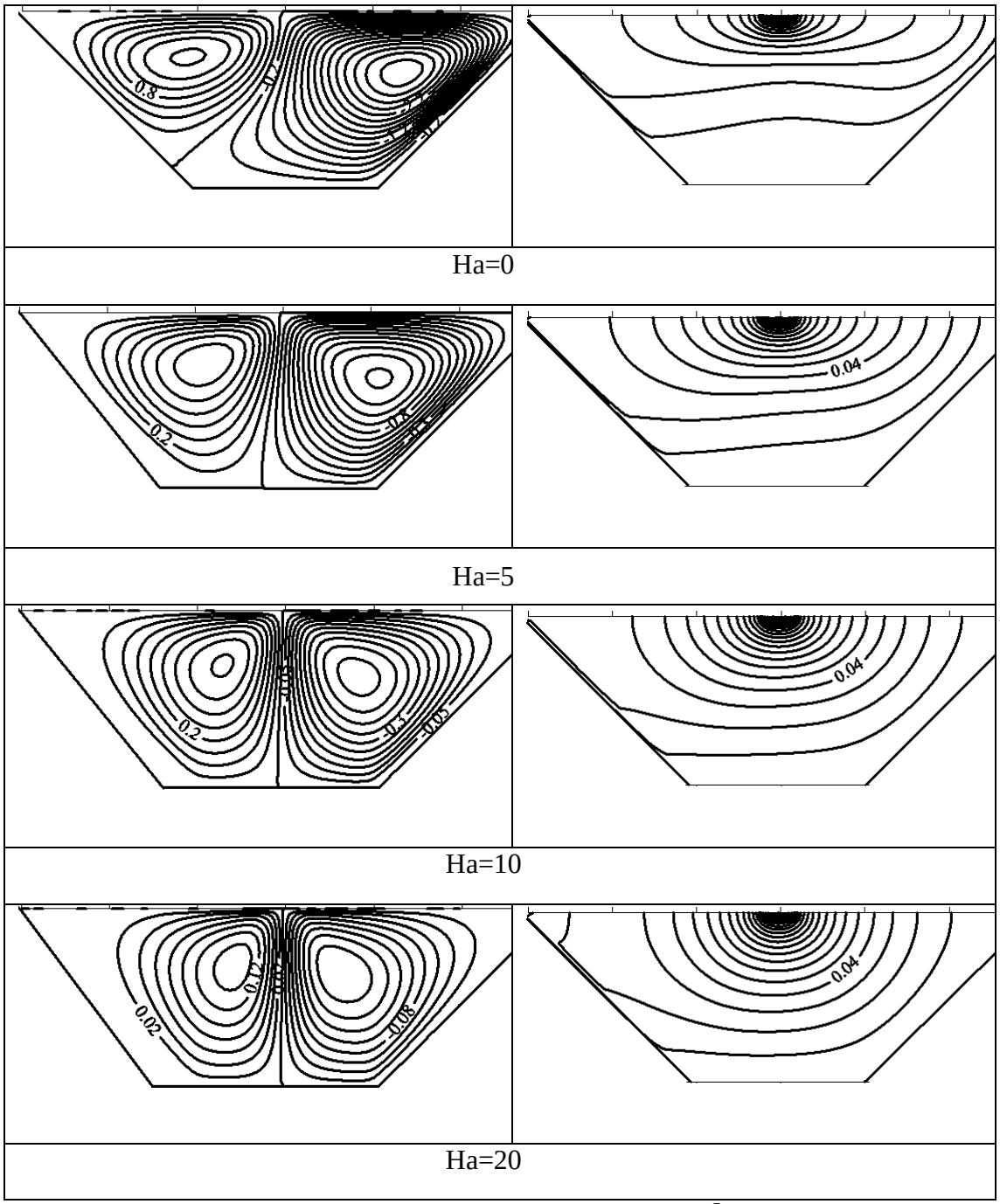

Fig.7 Streamlines (left) and isotherms (right) with Φ=0, Ra=10^5, B=0.2, D=0.5, φ=0.01.s

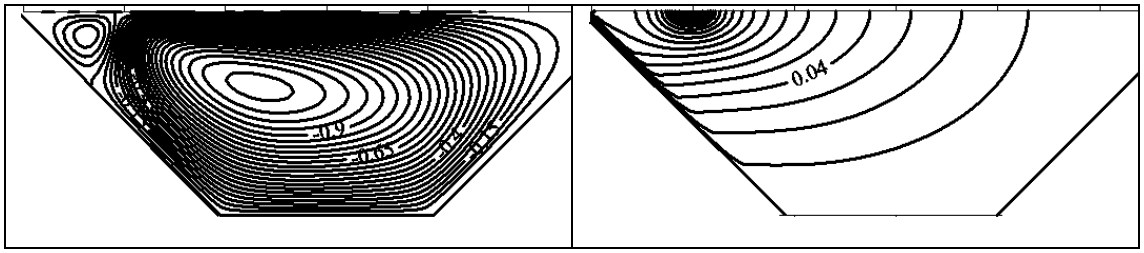

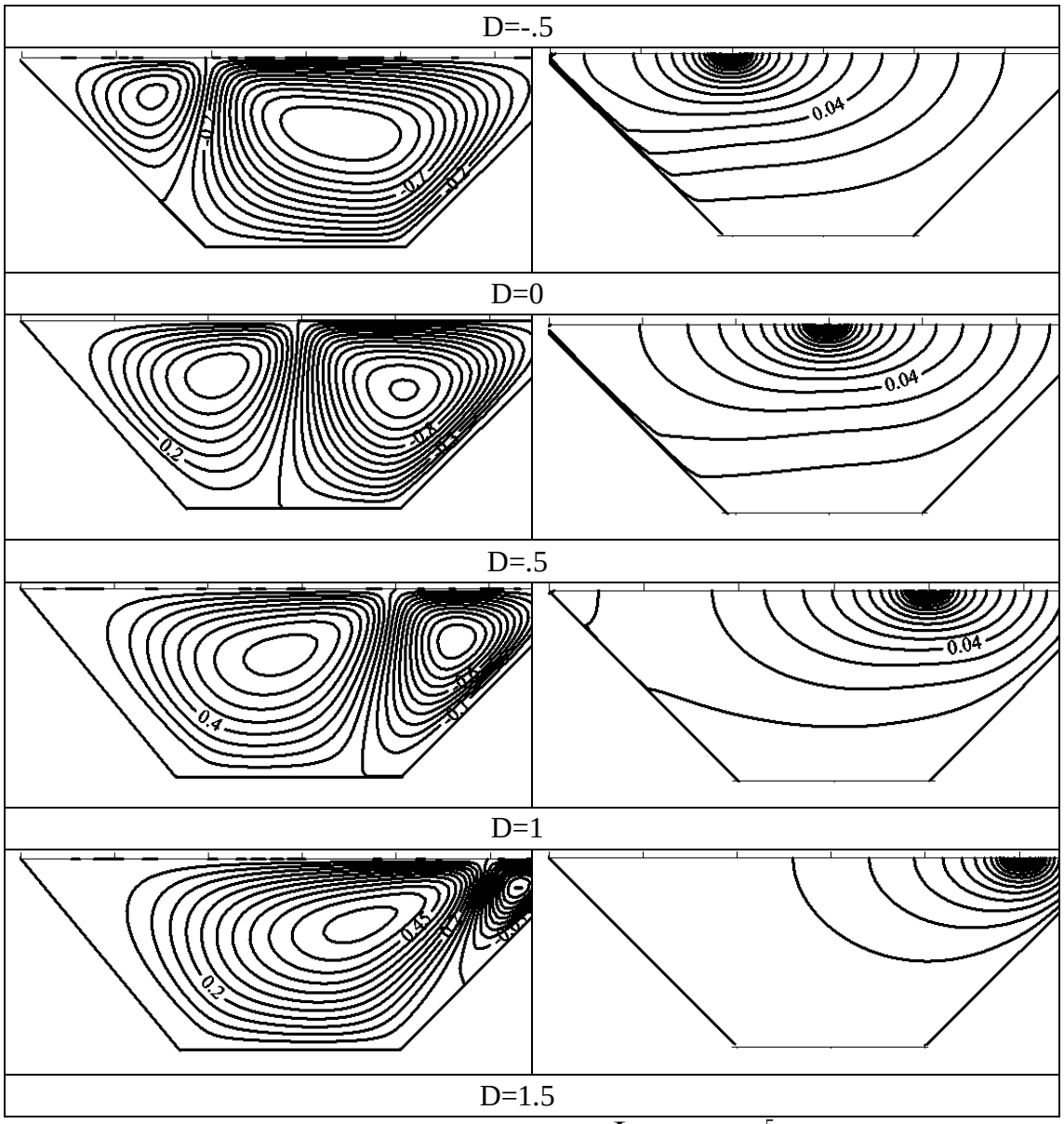

Fig.8 Streamlines (left) and isotherms (right) with Φ=0, Ra=10^5, B=0.2, Ha=5, φ=0.01.

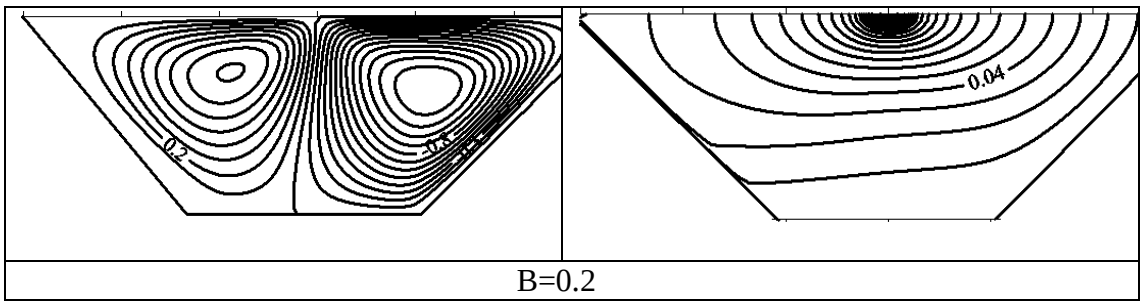

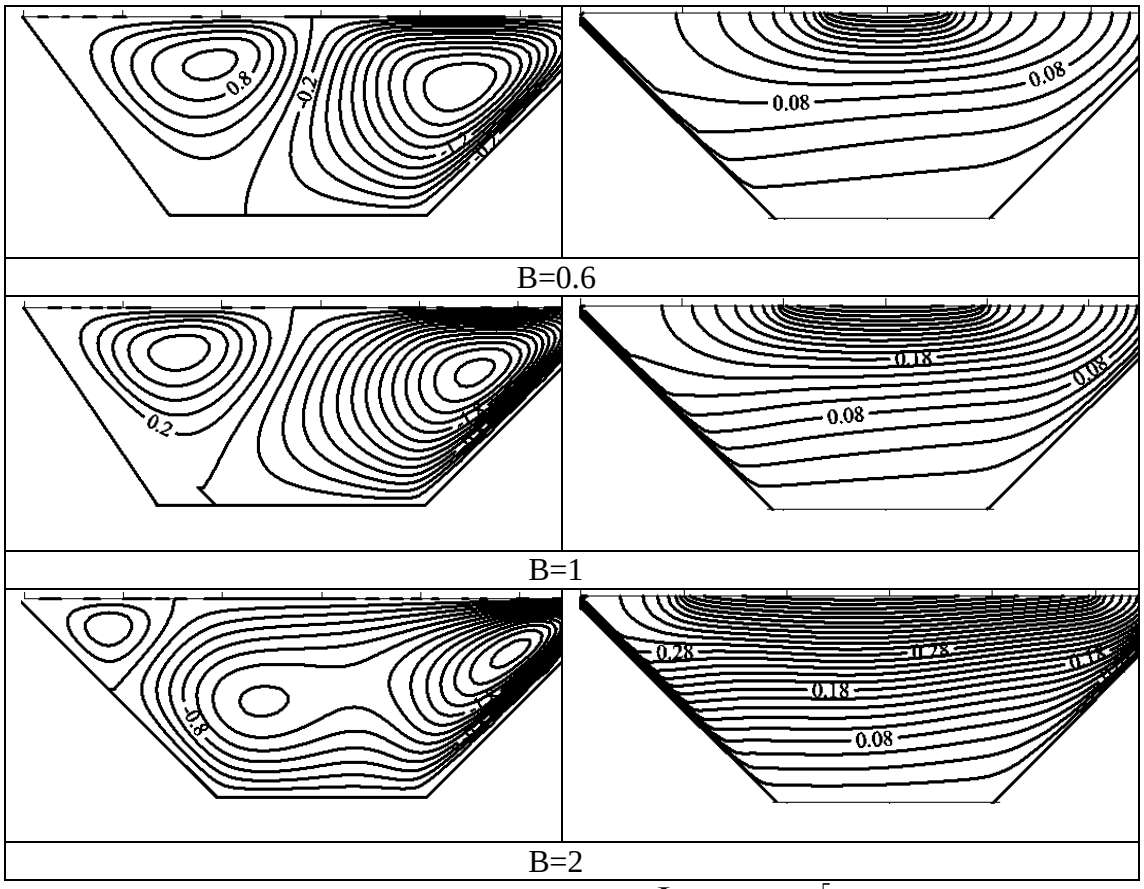

Fig.9 Streamlines (left) and isotherms (right) with Φ =0, Ra=10^5, D=0.5, Ha=5, φ =0.01.

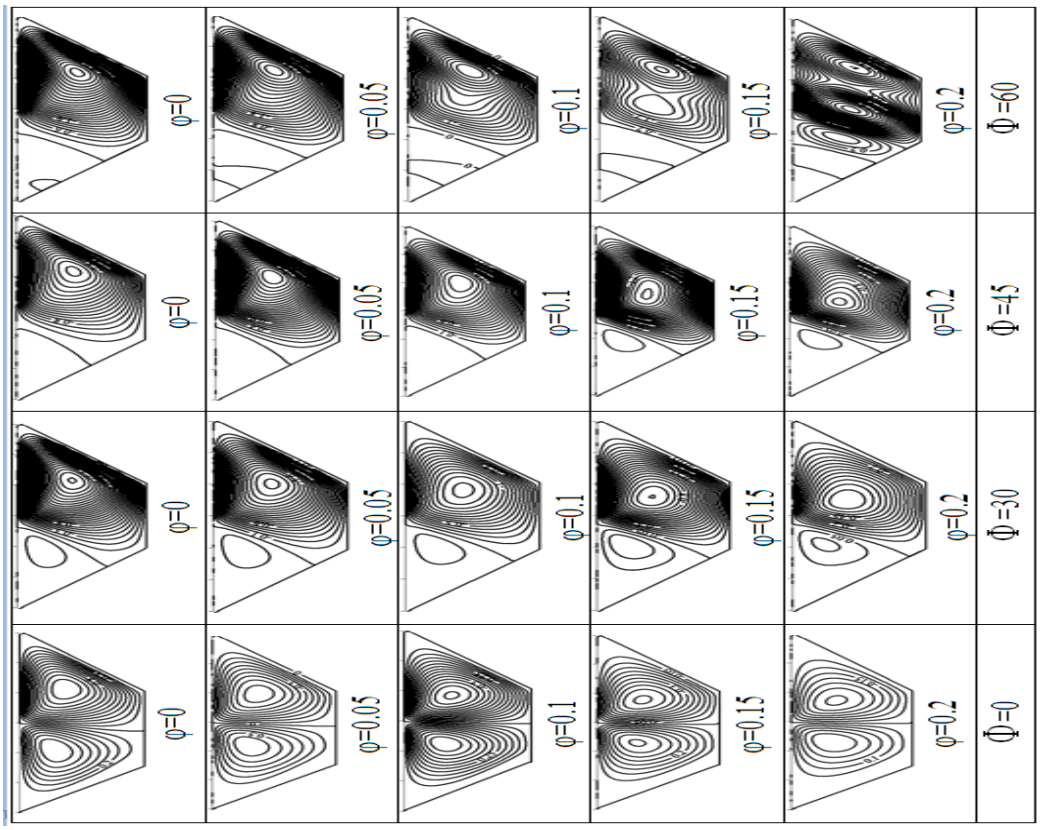

Fig.10 Streamlines B=0.2, Ra=10^5, D=0.5, Ha=5

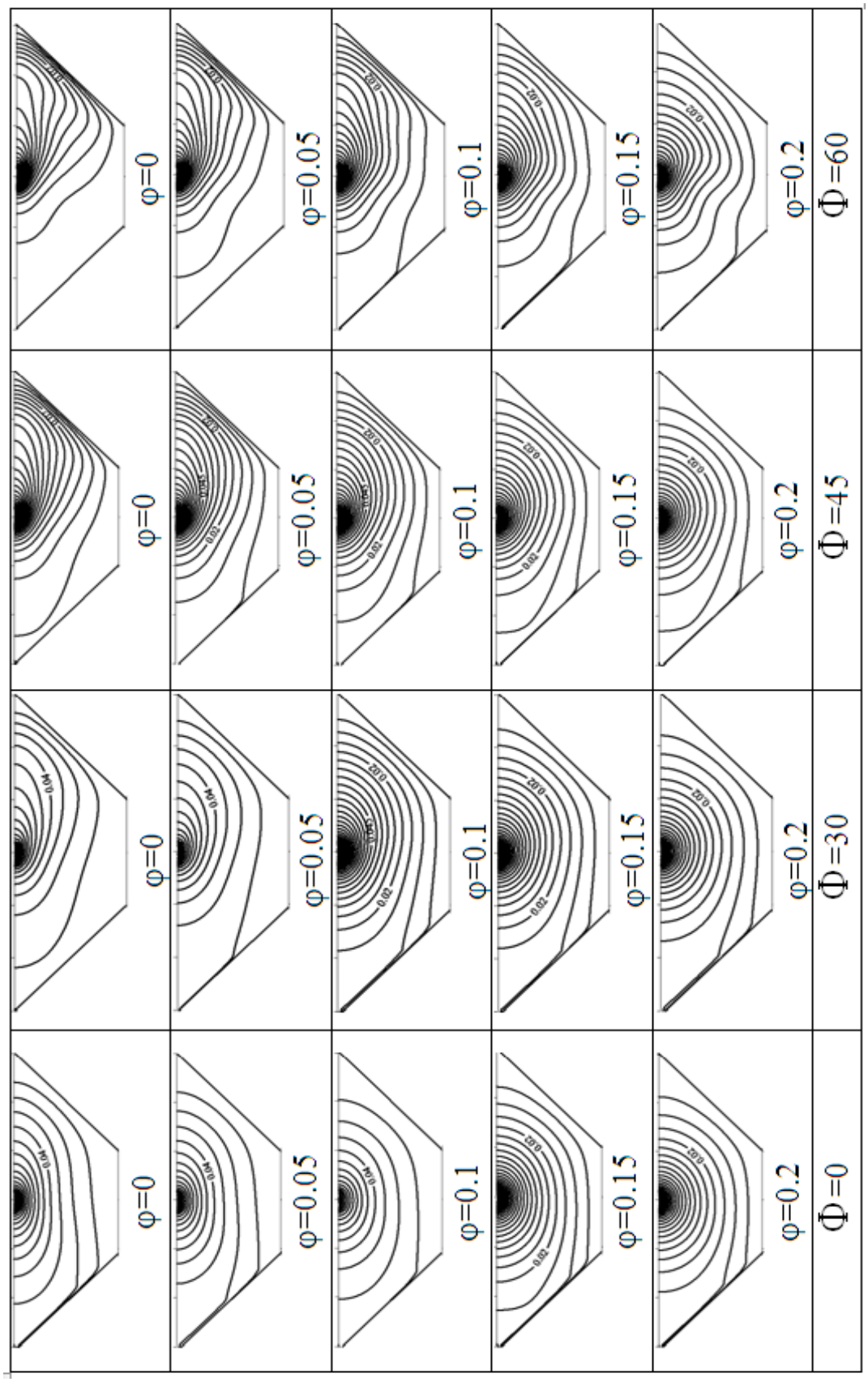

Fig 11 Isotherms B=0.2, Ra=10^5, D=0.5, Ha=5.

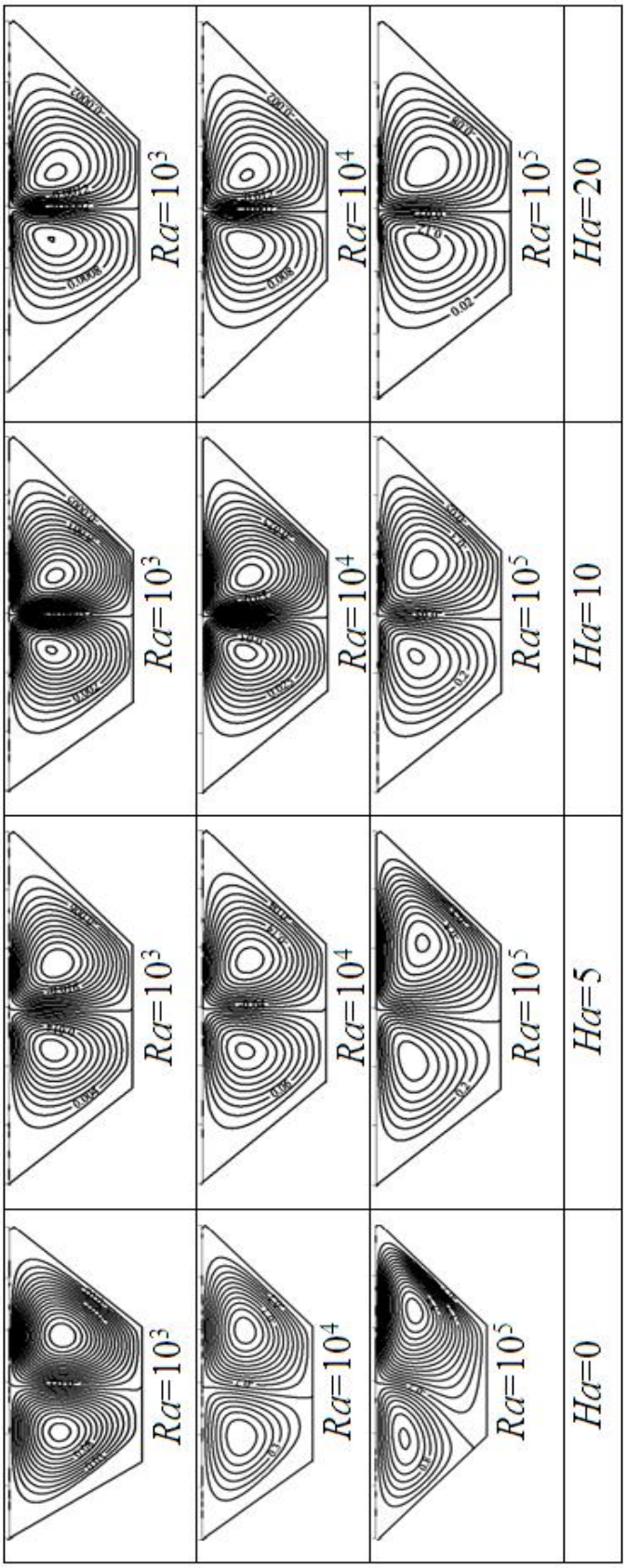

Fig 12 Streamlines B=0.2, Φ=0, D=0.5, φ=0.01.

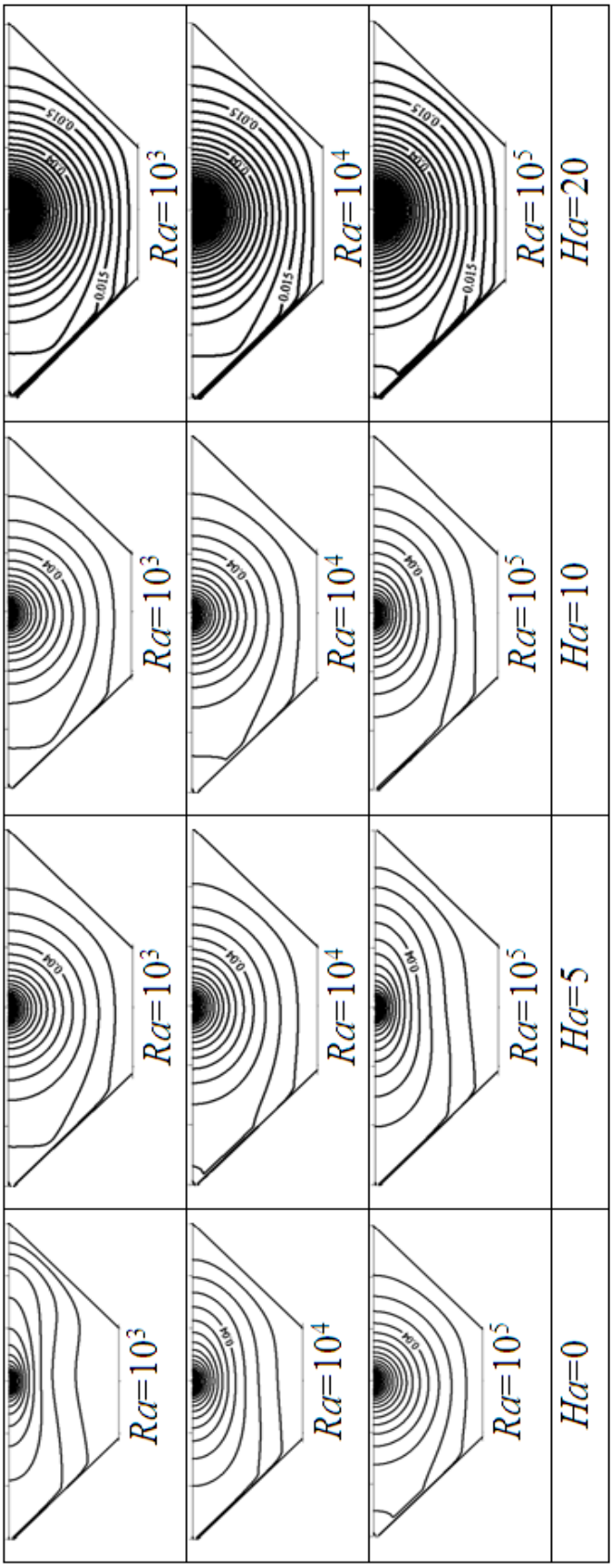

Fig.13 Isotherms B=0.2, Φ=0, D=0.5, φ=0.01.

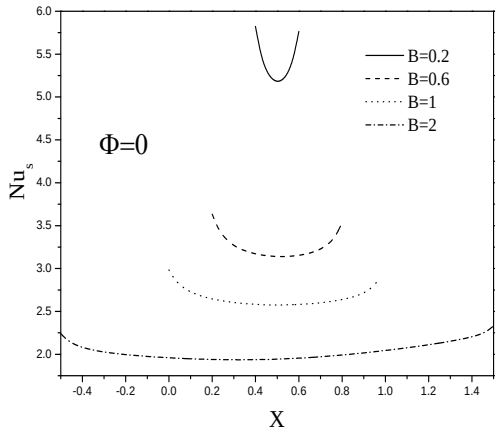

Fig. 14 Variation of local Nusselt number along the heat source for different heat source lengths.

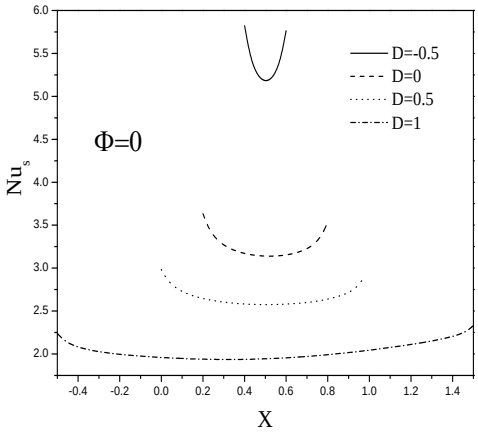

Fig. 15 Variation of local Nusselt number along the heat source for different heat source locations.

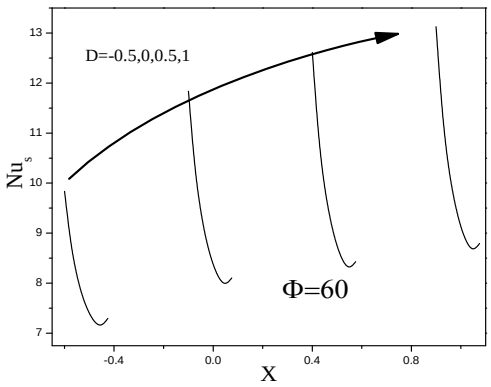

Fig. 16 Variation of local Nusselt number along the heat source for different heat source lengths.

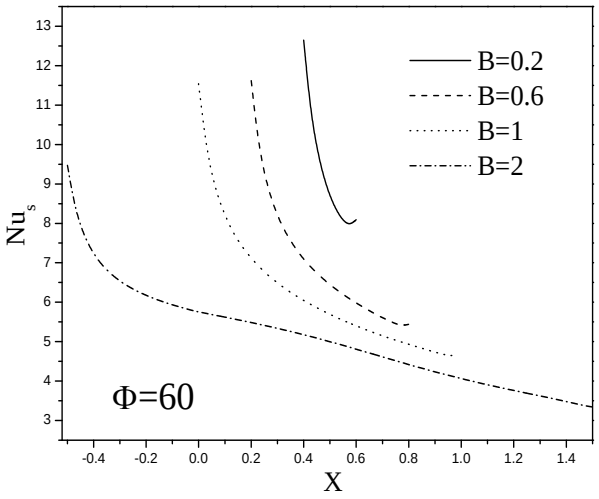

Fig. 17 Variation of local Nusselt number along the heat source for different heat source lengths.

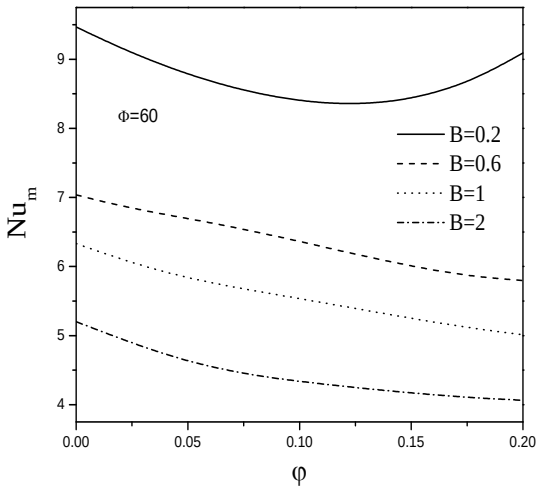

Fig. 18 The effect of distinct heat source lengths on variation of average Nusselt number with solid volume fraction.

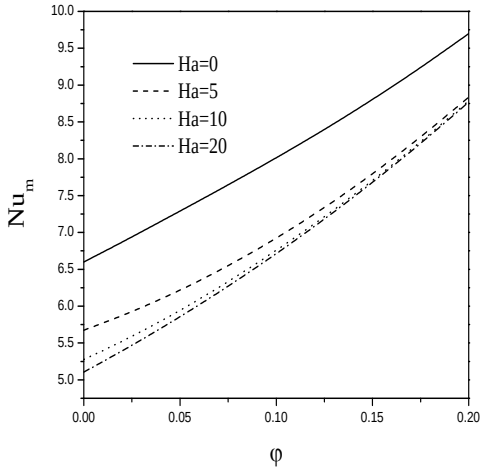

Fig. 19 The effect of distinct Hartmann numbers on variation of average Nusselt number with solid volume fraction.

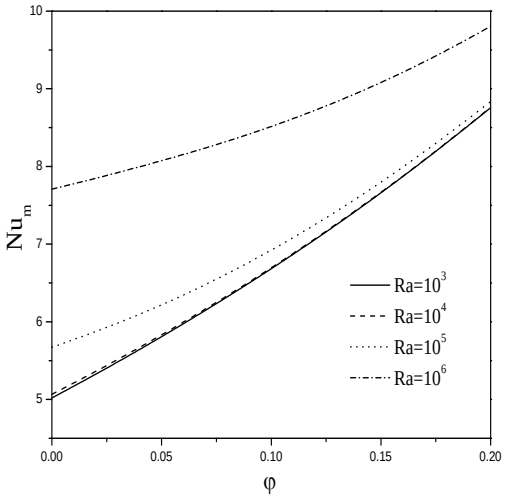

Fig. 20 The effect of distinct Raylei-gh numbers on variation of average Nuss-elt number with solid volume fraction.

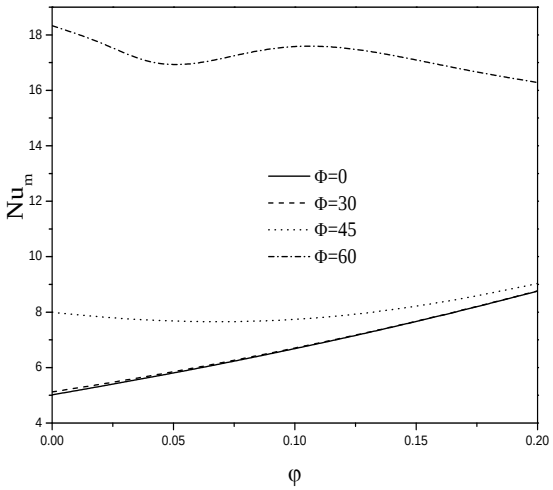

Fig. 21 The effect of various tilted positions on variation of average Nusselt number with solid volume fraction.

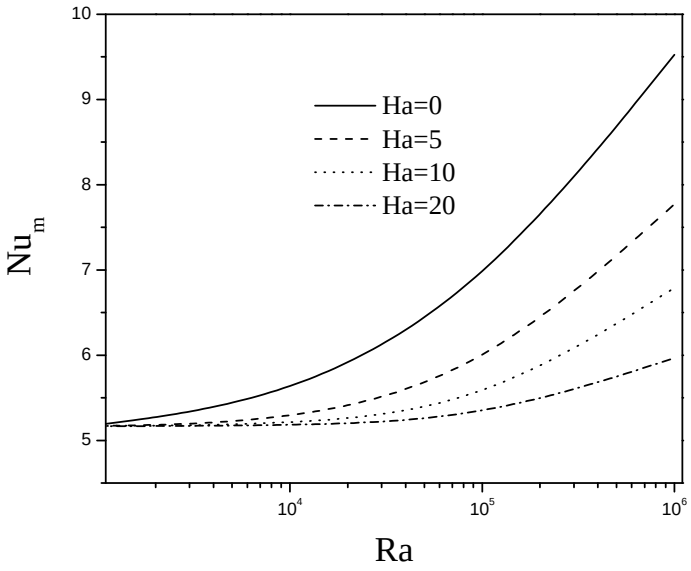

Fig. 22 The effect of distinct Hartmann numbers on variation of average Nusselt number for different Rayleigh numbers.

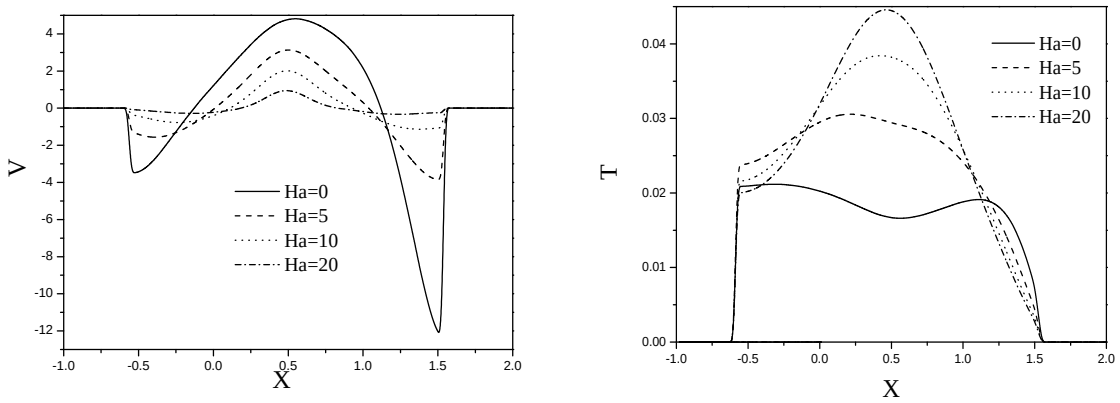

(a) (b)

Fig. 23 The effect of distinct Hartmann numbers on variation of (a) vertical velocity and (b) dimensionless temperature along the middle horizontal axis.

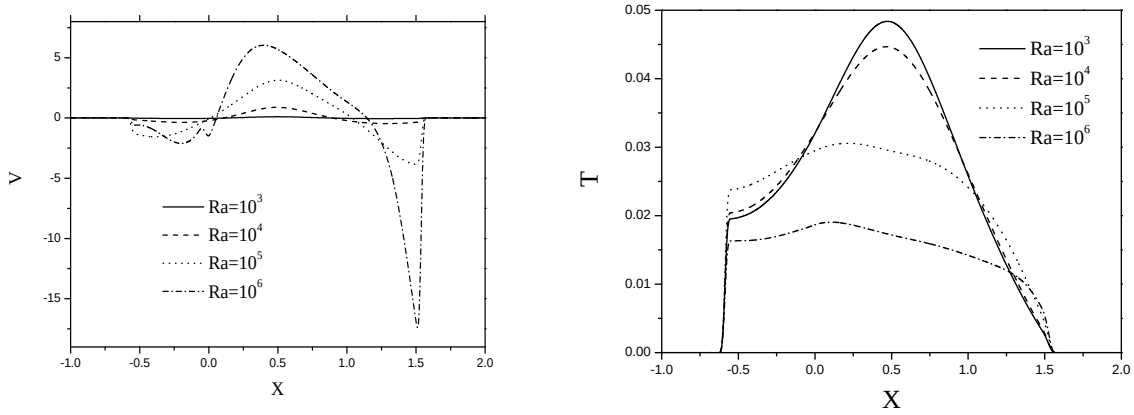

(a) (b)

Fig. 24 The effect of distinct Hartmann numbers on variation of (a) vertical velocity and (b) dimensionless temperature along the middle horizontal axis.

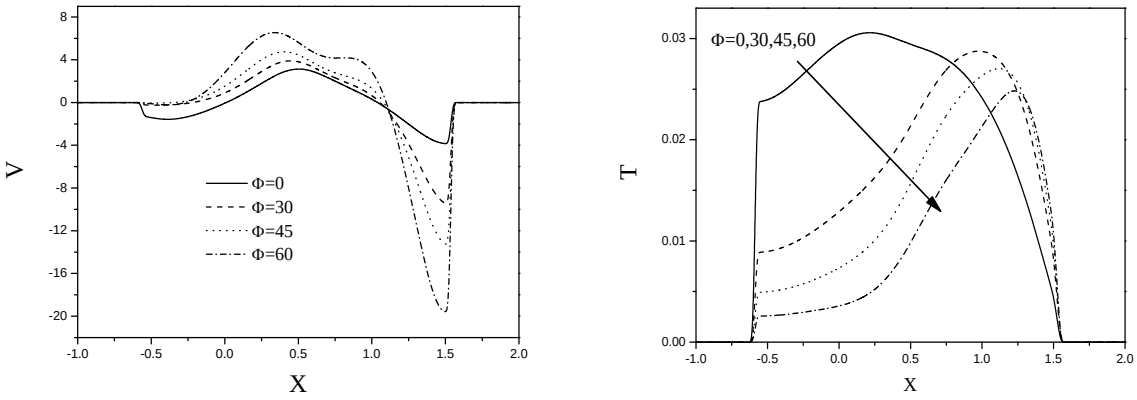

(a) (b)

Fig. 25 The effect of different tilted positions on variation of (a) vertical velocity and (b) dimensionless temperature along the middle horizontal axis.

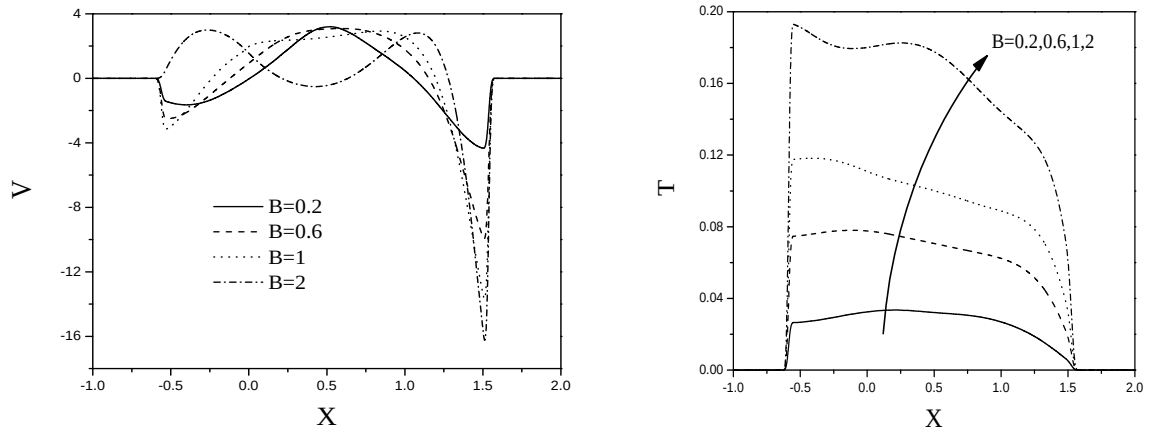

(a) (b)

Fig. 26 The effect of distinct heat source lengths on variation of (a) vertical velocity and (b) dimensionless temperature along the middle horizontal axis.

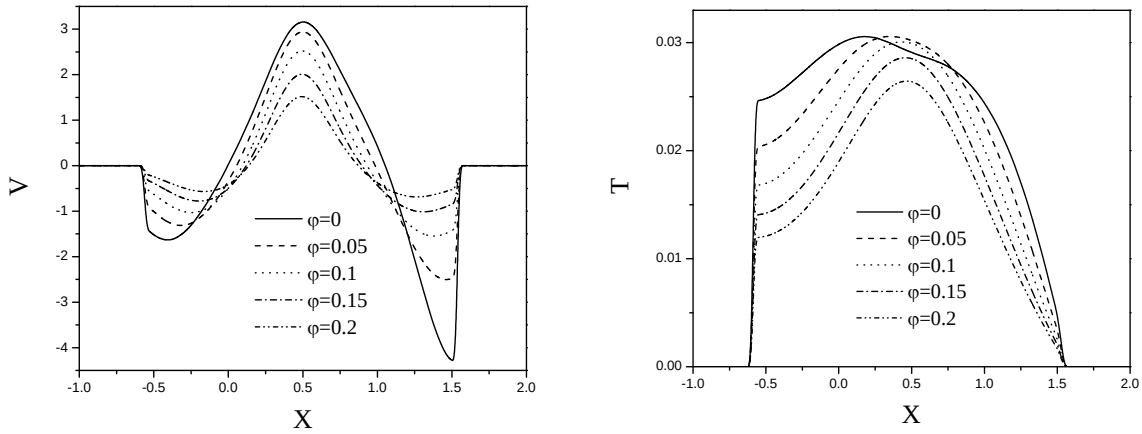

(a) (b)

Fig. 27 The effect of distinct solid volume fractions on variation of (a) vertical velocity and (b) dimensionless temperature along the middle horizontal axis.